Drought variability in eastern Mongolian Plateau and its linkages to the large-scale climate forcing

Guang Bao · Yu Liu · Na Liu · Hans W. Linderholm

Abstract A robust regional tree-ring chronology with a span of 1819–2009 was developed for the Hulun Buir steppe, China, a region in the eastern edge of the Mongolian Plateau. This chronology exhibited significantly positive correlation with precipitation in June, and negative correlations with temperature from April to September except for May. Highest correlation was found between tree rings and the average April–August standardized precipitation evapotranspiration index (SPEI), suggesting that pines growth strongly respond to the seasonal drought conditions. Accordingly, the average April–August SPEI reconstruction was performed for the period 1854–2009, explaining 45.5 % variance of the calibration period 1953–2009. New reconstruction shows some synchrony with regional-scale events found in other reconstructions to the west Mongolian Plateau. The recent droughts in late 1990 to present are not unusual in the context of the past several centuries. Spectrum analyses suggested that the average April–August SPEI variations, especially severe droughts in the late 1870s-early 1880s, 1920s and since the late 1990s could be associated with large-scale climate forcing, such as the El Niño-Southern Oscillation, the Pacific Decadal Oscillation and the summer North Atlantic Oscillation. Significant teleconnections indicated drought variability during the past several centuries in eastern Mongolian Plateau existed close connections with large-scale synoptic features.

G. Bao (✉) · N. Liu
Key Laboratory of Disaster Monitoring and Mechanism
Simulating of Shaanxi Province, Baoji University of Arts
and Sciences, Baoji 721013, Shaanxi, China
e-mail: baoguang@ieecas.cn

G. Bao · Y. Liu (✉)
State Key Laboratory of Loess and Quaternary Geology,
Institute of Earth Environment, Chinese Academy of Sciences,
Xi'an 710075, China
e-mail: liuyu@loess.llqg.ac.cn

Y. Liu · N. Liu
Department of Environmental Science and Technology,
School of Human Settlements and Civil Engineering,
Xi'an Jiaotong University, Xi'an 710049, China

H. W. Linderholm
Regional Climate Group, Department of Earth Sciences,
University of Gothenburg, Box 460, 405 30 Gothenburg, Sweden

1 Introduction

Drought as a recurring extreme climate event not only plays an important role for agriculture, water resources and ecosystems (Dai 2011), but also profoundly affects millions of people around the world every year (Wilhite 2000). Recent studies indicate that severe drought with more frequency and persistent duration may be somewhat due to the increasing intensity of global warming (e.g. Cook et al. 2004; Dai et al. 2004; Dai 2011; Liu et al. 2013; Song and Liu 2011; Trenberth et al. 2004). The extreme four-year drought extending from 1999 to 2002 occurred in northern China (Zou et al. 2005) and Mongolia (Davi et al. 2006, 2013; Pederson et al. 2013), as well as in 2005 (China Daily, 12 August 2005) and 2009 (China Daily, 13 August 2009; Davi et al. 2013) are such cases, causing large economic and societal losses (Batima 2006; Zhang and Gao 2004). For instance, in

Inner Mongolia, China, the harsh drought of 2001 hampered 60×10^4 ha of planting area and caused great damage to the yield from 297×10^4 ha and $5,733 \times 10^4$ ha of crops and pasture, respectively (http://www.weather.com.cn/zt/kpzt/1244064.shtml). For without enough rain from late July to middle August, in 2005, camels' humps had shrunk as drought scorched the grasslands where many goats had already died of thirst in Alxa League in Inner Mongolia and bodies of dead goats also had be seen along the roads in Ningxia Hui autonomous region (http://www.chinadaily.com.cn/english/doc/2005-08/12/content_468265.htm). In 2009, a massive drought appeared in northeast China, where rainfall had fallen by 50–90 % since July compared to normal years. This dry spell had affected 10.8 million acres of farmland and caused drinking water difficulties for 810,000 people in the provinces of Heilongjiang, Jilin and Liaoning, as well as the Inner Mongolia (http://www.chinadaily.com.cn/cndy/2009-08/13/content_8562996.htm). The consistent drought trend appeared in Mongolia and Inner Mongolia, China may suggest the similar hydroclimatic pattern reflected by variations of drought in Mongolian Plateau to some degree.

Limited meteorological data (most back to 1950s) impede our understanding of the possible processes and mechanisms of drought variability within a long-time scale over this large region. However, the long-term records based on tree rings have been proved the values of extending the short and sparse meteorological records, as well as of serving to evaluate the impacts of various factors over time (e.g. Cook et al. 2010; D'Arrigo et al. 2000, 2001; Davi et al. 2006, 2009, 2010; Pederson et al. 2001, 2013), including the Kherlen River basin in eastern Mongolia (Davi et al. 2013; Pederson et al. 2001), the Selenge River basin in central Mongolia (Davi et al. 2006), far western Mongolia (Davi et al. 2009), the Yeruu River basin in northern Mongolia (Pederson et al. 2013), as well as the whole Mongolia (Davi et al. 2010). Nevertheless, studies conducted in the eastern edge of the Mongolian Plateau are quite few (Bao et al. 2012; Chen et al. 2012; Liu et al. 2009). The purposes of this study were (1) to reconstruct the average April–August drought variability in the last two centuries for Hulun Buir region, eastern edge of the Mongolian Plateau, and (2) to explore the linkage between the extreme drought events variations in central and eastern Mongolian Plateau and large-scale climate forcing conditions. Our results are expected to further understand the characteristics of extreme drought events over a large spatial–temporal scale.

2 Data and methods

2.1 Study area and climate

Hulun Buir steppe, located in the eastern region of Mongolian Plateau, China, is a remote inland zone dominated by a nomadic culture (Fig. 1). It is also situated in a transitional zone between semiarid and arid conditions, monsoon and non-monsoon climates, as well as agricultural and pasture lands (Fu et al. 1998; Zhao et al. 2002). The climate is featured by low rainfall, extreme temperature, strong winds, high evaporation, and poor soil quality (Zhu et al. 2003). Seasonal dry/cold and wet/warm conditions are strongly influenced by the intrusion of dry, cold air masses from high latitudes in winter and warm, humid air masses from low-latitude oceans in summer (Chinese Academy of Sciences 1984). Droughts occur frequently in each season, especially during spring and summer (Shen 2008).

Meteorological data of Hailar (119°45′E, 49°13′N, 610 m a.s.l.) and Aershan (119°57′E, 47°10′N, 1,027 m a.s.l.) stations were obtained from the China Meteorological Data Sharing Service System (http://cdc.cma.gov.cn), including the monthly precipitation, monthly mean temperature, maximum temperature and minimum temperature for the period of 1953–2008. As averaging meteorological records from more stations could decrease the small-scale noise or stochastic components and represent broader regional climatic conditions (Chen et al. 2012; Davi et al. 2006), we used the arithmetical averaged data set from the Hailar and Aershan stations for further analysis. Annual mean temperature and total precipitation are –1.99 °C and 399 mm, respectively. The highest and lowest monthly mean temperature is 18.37 °C in July and –25.45 °C in January. Distributions of temperature and precipitation were shown in Fig. 2.

2.2 Tree-ring data

Tree-ring samples were collected from three sites of old growth *Pinus sylvestris* var. *mongolica* forest (Fig. 1; Table 1). Two sites were located in southern Hulun Buir steppe, i.e. NGNE (119°22.037′–119°23.788′E, 47°59.539′–47°59.851′N, 760–790 m a.l.s.) and BRT02 (119°28.981′–119°29.551′E, 47°49.894′–47°50.381′N, 894–915 m a.l.s.) (Bao et al. 2012), and the third site HLBE (119°43′E, 49°12′N, 450–600 m a.l.s.) lies in the northern (Liu et al. 2009). All the cores of ring-width samples were processed (including dried, mounted and surfaced), measured (with a precision of 0.01 mm) and cross-dated following standard dendrochronological procedures (Cook and Kairiukstis 1990; Fritts 1976). Quality control for cross-dating was carried out using COFECHA (Holmes 1983). Chronologies were developed for each site using the program ARSTAN (Cook 1985). To retain as much of the low-frequency signal as possible, each ring-width measurement series was detrended conservatively by fitting negative exponential curves or linear regression curves. The individual index series were then combined into a single chronology by computing a biweight robust estimate of the mean (Cook and Kairiukstis 1990).

Fig. 1 Rectangles indicate this study area (*red*), the Kherlen River basin (*green*, Pederson et al. 2001) and the Selenge River basin (*blue*, Davi et al. 2006) (*top*); locations of the three sampling sites, two meteorological stations and one grid SPEI point (*bottom*)
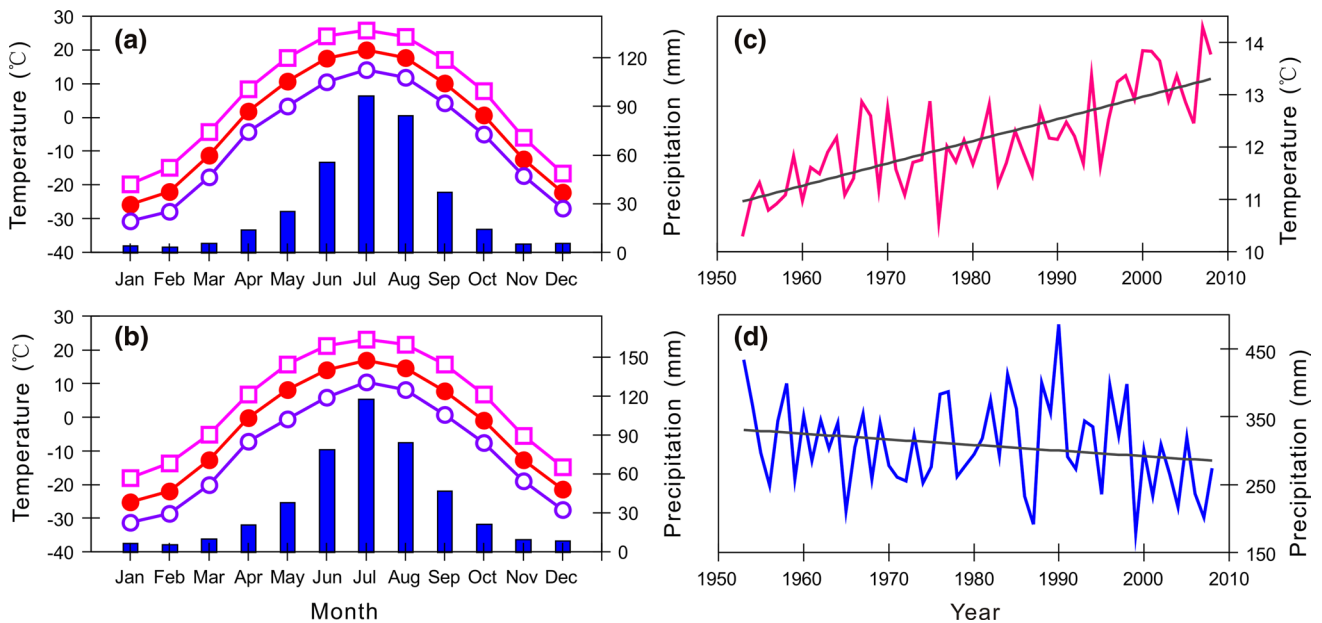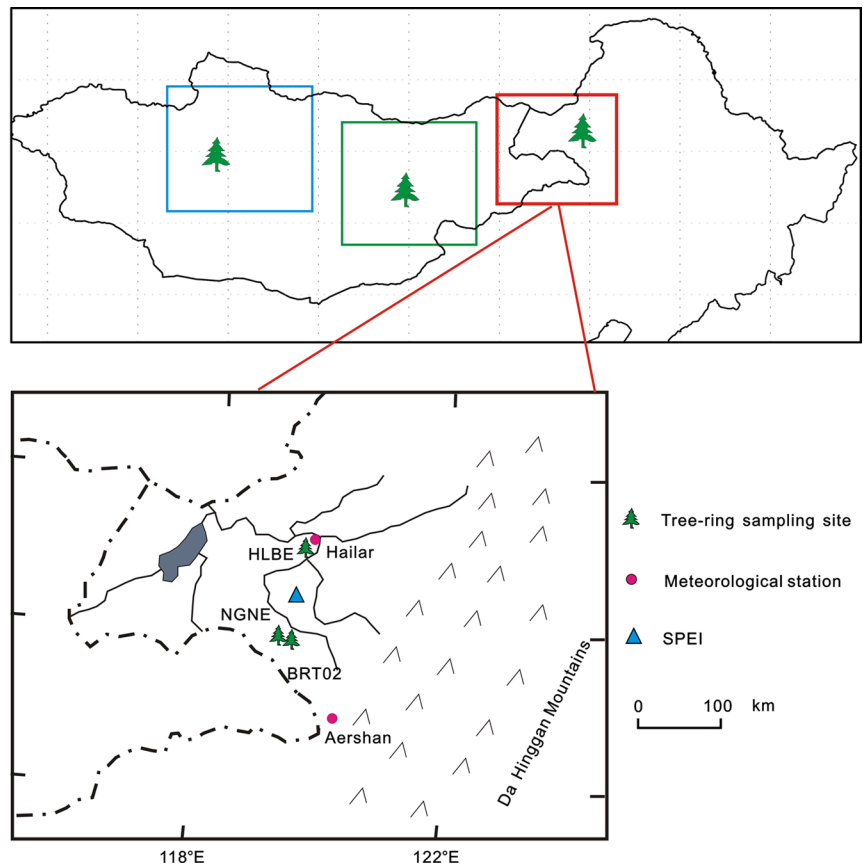
Fig. 2 Monthly mean temperature (*filled dot*), mean maximum temperature (*unfilled rectangle*), mean minimum temperature (*unfilled dot*) and sum of precipitation (*filled bar*) for **a** Hailar, **b** Aershan meteorological stations; variations of the mean temperature of April–August (**c**) and total precipitation of April–August (**d**) for the averaged data of Hailar and Aershan meteorological stations (1953–2008)

Table 1 Characteristics of the three sampling sites and statistics of standard chronologies

Site	Chronology span	Rbt	MS	SD	AC1	EPS	Period of SSS > 0.85	Number of cores
NGNE	1843–2009	0.415	0.19	0.22	0.49	0.96	1873–2009	67
BRT02	1842–2009	0.288	0.15	0.22	0.62	0.87	1914–2009	35
HLBE	1819–2003	0.296	0.23	0.36	0.64	0.91	1887–2003	40
NB02HSTD	1819–2009	0.387	0.19	0.14	0.61	0.97	1849–2009	124

NB02HSTD regional tree-ring width standard chronology composed of the three sampling sites, Rbt correlation coefficient between trees, MS mean sensitivity, SD standard deviation, AC1 first order autocorrelation

Fig. 3 The regional tree-ring standard chronology (NB02H-STD) (*top*), the statistics of the running Rbar (running for based upon a 30-year window lagged 15 years) and the running expressed population signal (EPS) (*middle*) and the sample depth (*bottom*). The reliable portion of the chronology is determined by the EPS value >0.85
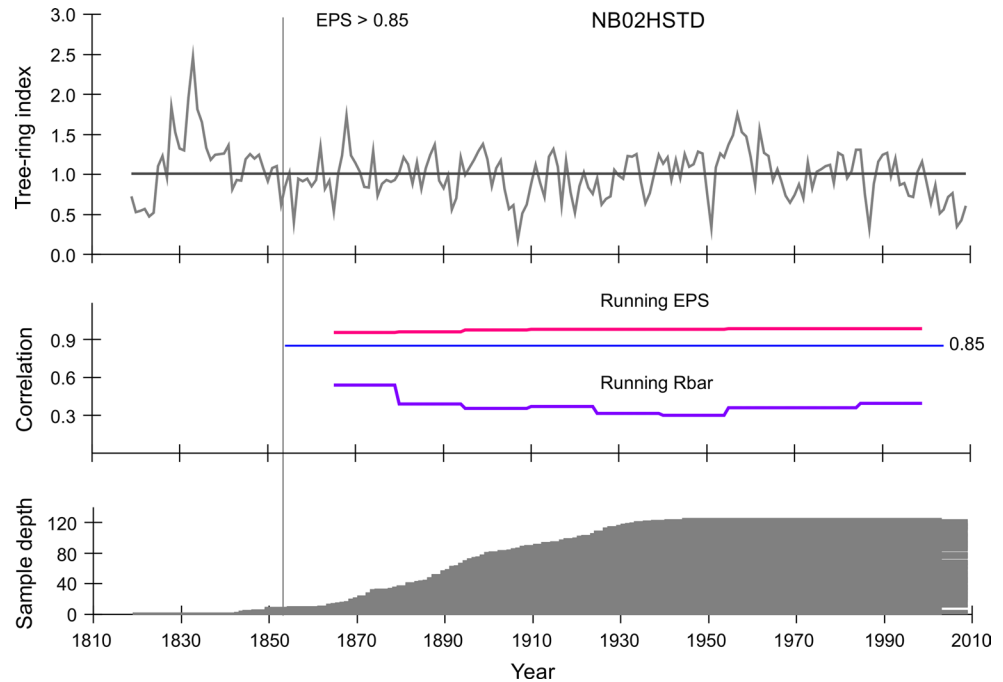
The Statistical features of each standard chronology (STD) were shown in Table 1. Subsample signal strength (SSS) was employed to assess the replication in the early years of the chronology (Wigley et al. 1984). The significant correlations (at the level $p < 0.0001$) between the three site-chronologies were 0.697 (NGNE and BRT02, 1886–2009), 0.595 (NGNE and HLBE, 1886–2003) and 0.545 (BRT02 and HLBE, 1886–2003) since the year 1886AD of SSS >0.75 for BRT02, and the first principal component explained 73.4 % of the total variance, a regional chronology (NB02HSTD) was developed using the total 124 samples from three sites, after excluding cores with worse correlations with master series (Table 1). The variance of the chronology was stabilized with the Rbar-weighted method outlined in Osborn et al. (1997) to reduce the effects of changing sample size. The NB02HSTD spans the period from 1819 to 2009, and the reliable interval with the SSS >0.85 is 1849–2009. The latter extended at least 24-year long comparing with each site-chronology (Table 1). Running expressed population signal (EPS) and running Rbar (moving correlations among

series) values were generally high (Fig. 3), indicating reliable chronology signal strength through time (Wigley et al. 1984). The following analyses were only based on the reliable portion of the chronology spanning from 1854 to 2009, which was suggested by the EPS value greater than 0.85 (Wigley et al. 1984).

2.3 SPEI data

A new drought index of the standardized precipitation evapotranspiration index (SPEI) was utilized in this study, which is based on precipitation and temperature data (Vicente-Serrano et al. 2010a). The SPEI has the advantages of combining the multitemporal nature of the standardized precipitation index (SPI) and the sensitivity of the Palmer drought severity index (PDSI) (Dai et al. 2004) to changes in evaporation demand caused by temperature fluctuations and trends. The SPEI has identified an increase in drought severity resulting from higher water demand caused by evapotranspiration under global

warming conditions (Vicente-Serrano et al. 2010a, b). The nearest grid data of SPEI (48°15′N, 119°15′E, 1952–2009) (Vicente-Serrano et al. 2010b) was abstracted for climate-growth response analyses.

2.4 Methods

Correlation analysis was applied to identify the relationship between tree-ring growth and climate factors during the observation period 1953–2009. Monthly mean precipitation, mean temperature, SPEI and PDSI from the previous October to current September were used. Climate variables of various seasons and their correlations with NB02HSTD were also tested. Linear regression analysis was utilized to reconstruct the average April–August SPEI. Split-sample method was applied to verify the skill of the regression model (Meko and Graybill 1995) and the statistics for model evaluation include Pearson's correlation coefficient (r), sign test (ST), reduction of error (RE), and coefficient of efficiency (CE). RE and CE are measures of shared variance between actual and estimated series, particularly CE is a more rigorous verification statistic, with a positive value suggesting that the reconstruction has encouraging performance (Cook et al. 1994, 1999). The average April–August SPEI reconstruction was evaluated for pluvial and drought characteristics, by using magnitude (sum of the departure values from the long-term median) and intensity (sum of the departure values from the median divided by the duration) of each events (2 years or greater) through time (Biondi et al. 2002; Davi et al. 2013; Gray et al. 2011; Pederson et al. 2013). To represent regional-scale climate signal variability, spatial correlation analyses were performed using the KNMI Climate Explorer (http://www.knmi.nl) and the datasets included CRU TS3.1 (Mitchell and Jones 2005), CSIC SPEI (Vicente-Serrano et al. 2010b) and NCDC ERSSTv3 (Smith et al. 2008). Wavelet analyses were performed using software (Torrence and Compo 1998).

3 Results

3.1 Climate-growth relationships

As shown in Fig. 4, tree rings were positively correlated with precipitation, particularly in June ($p < 0.05$), whereas significantly negatively with temperature from April to September, except for in May. Significant positive correlations between NB02HSTD chronology and SPEI existed in the same month as displayed with temperature, in addition significantly negatively with the previous December SPEI. On the seasonal scale in the current stem growth period, the highest correlation was appeared in the average April–August SPEI (r = 0.675, $p < 0.0001$, n = 57).

3.2 Reconstruction

Based on the growth-climate response relationship, the average April–August SPEI was reconstructed using a line regression model. All the statistics in the verification and calibration were listed in Table 2. Especially, the reduction of error (RE) and the coefficient of efficiency (CE),

Fig. 4 Correlations between NB02HSTD and monthly total precipitation (*black bar*) and monthly mean temperature (*cross bar*) for the averaged data of Hailar and Aershan meteorological stations (1953–2008) (*top*) and SPEI (*grey bar*) (1952–2009) (*bottom*) from previous October to current September. "+" refers to $p < 0.05$, "×" represents $p < 0.01$
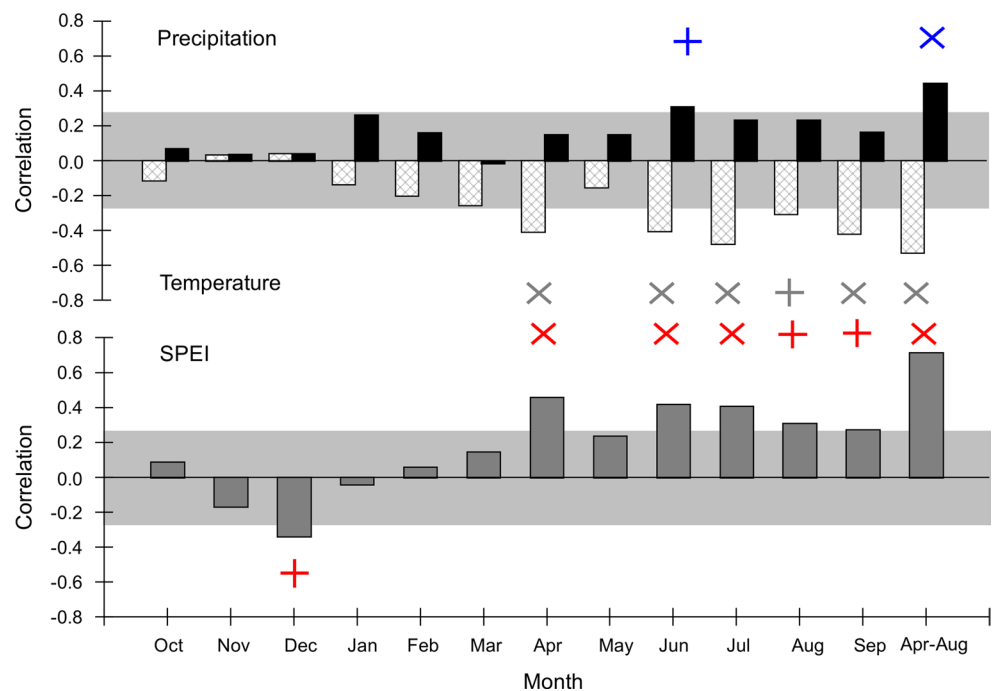
Table 2 Statistics of the split calibration and verification model for the average April–August SPEI reconstruction for the Hulun Buir steppe

Calibration				Verification				
Time span	r	R^2	F	Time span	r	RE	CE	ST
1953–1980	0.594[a]	0.353	14.170[a]	1981–2009	0.632[a]	0.537	0.225	21+/8−[b]
1981–2009	0.632[a]	0.400	17.972[a]	1953–1980	0.594[a]	0.601	0.210	17+/11−
1953–2009	0.675[a]	0.455	45.966[a]					

RE reduction error, *CE* coefficient of efficiency, *ST* sign test

[a, b] The significance level of 0.001 and 0.05, respectively

Fig. 5 (*Top*) Comparison between observed (*blue line*) and reconstructed average April–August SPEI (*pink line*) for the period 1953–2009, (*bottom*) reconstructed average April–August SPEI (*grey thin line*) with its 10-year low-pass filter (*pink bold line*) and its average value (*horizontal line*) for the period 1854–2009
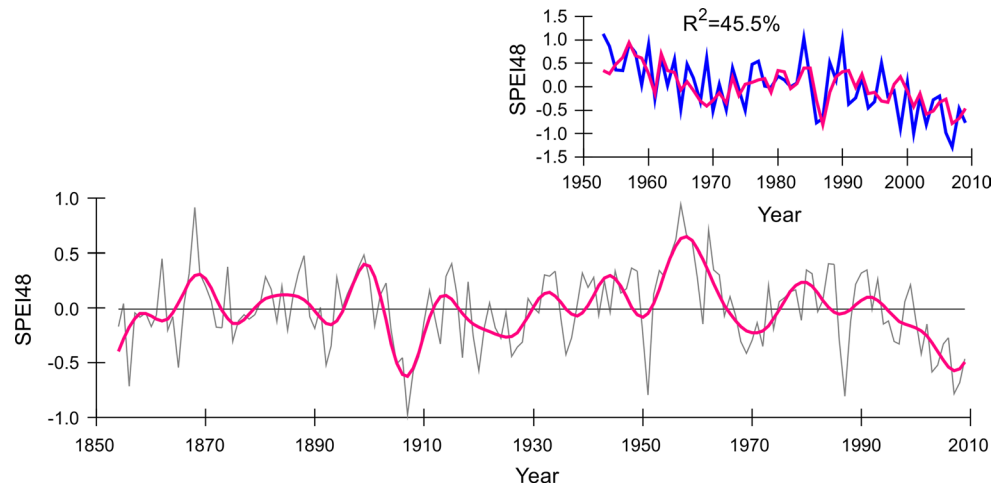
the two most rigorous tests for model validation, were positive for both verification intervals confirming acceptable reconstruction reliability (Cook and Kairiukstis 1990; Fritts 1976).

Therefore, the transfer function was designed for the reconstructed average April–August SPEI (RECSPEI48) and tree-ring chronology (NB02HSTD) as follows:

$$\text{RECSPEI48} = 1.228 \times \text{NB02HSTD} - 1.208, \quad (1)$$

The percentage of the variance explained by NB02HSTD in this model (1) was 45.5 % (44.6 % after adjustment for the loss of degrees of freedom) for the calibration period 1953–2009. The comparison indicates close agreement between the observation and the reconstructed series during the calibration period (Fig. 5 top). The variations at both high and low frequencies for the reconstruction of the average April–August SPEI for 1854–2009 were shown in Fig. 5 (bottom).

4 Discussion

4.1 Signal of the average April–August SPEI

Drought stress is thought to be the main climate limitation for the *Pinus sylvestris* var. *mongolica* radial growth in the Hulun Buir steppe. This pattern can be inferred from the positive correlations with rainfall and negative correlations with temperature (Cai et al. 2010; Fang et al. 2012; Song and Liu 2011). Significant correlations between NB02H-STD and SPEI confirmed such drought sensitive climate-growth relationship. Indeed, cambial cell division begins in early May in northern China (Liang et al. 2009). However, recently, Liu et al. (2013) found the ecologically significant shift in mean daily temperature from below 0 °C to above 0 °C occurs about a month earlier, in early April in northern China and late April in southern Siberia. Climate variations may enhance the sensitivity of tree growth to drought conditions at the semi-arid areas. Temperature and precipitation in May did not show significant correlations with tree-ring index that could be due to the co-variation of meltwater and increase rain reducing the negative effect of high rate of evapotranspiration produced by enhancing temperature. Seeds maturation and trees dormancy of *Pinus sylvestris* var. *mongolica* occur in late September and October, respectively (He et al. 2005; Zhao and Li 1963). He et al. (2005) found that the latewood width index of *Pinus sylvestris* var. *mongolica* existed significant correlation with the averaged growing season Normalized Difference Vegetation Index (from May to September) which was driven by temperature in Mohe, a location more than 200 km north of our study area. However, ring width

formation of relict Chinese pine at its northern natural distribution limit in north china is completed in August (Liang et al. 2009) and the same stem activity has been revealed by the Populus trees in the Heihe River basin in northcentral China (Xiao et al. 2014). Though the species are different, the similar pattern of the cambial activity could be decided by the same arid-semiarid environment at these study regions. It is reasonable for us to reconstruct the variations of average April–August SPEI, although significant correlations exist in September between climate factors and tree rings. The climate-growth pattern in this study is consistent with the results of Liu et al. (2013), who demonstrated that drought in spring and summer of the growth year had strong influences on tree growth at semi-arid region in Inner Asia. That means the signal of average April–August SPEI may response to a large regional moisture condition.

4.2 Extreme events and drought variations

The mean value and standard deviation (SD) of the entire April–August SPEI reconstruction for 1854–2009 were −0.01 and 0.341, respectively. Extremely wet years are identified with a value >mean + 1 SD (= 0.331) and an extremely dry year as a year with a runoff <mean−1 SD (= −0.351). Based on these criteria, 22 extremely dry years and 23 extremely wet years occurred during the reference period. These years accounted for 14.1 and 14.7 % of the whole period, respectively (Table 3). The five driest years (<2 SD) were 1907, 1987, 1951, 2007 and 1856, and several missing rings appeared in 1907, 1987 and 1951. The three wettest years (>2 SD) were 1957, 1868 and 1962. Actually, the influence of extremely dry/wet years (events) tended to cover a large region. For instance, extremely dry years of 1907 (<2 SD), 1987 (<2 SD), 1865 (<1 SD) and 1892 (<1 SD) were identified as the top ten driest in the tree-ring-based rainfall reconstruction for Honghuaerji for 1806–2007 (Chen et al. 2012). The year 1987 (<2 SD) was recorded by many hydrological stations in the Hulun Biur region, including the Yiminmuchang, Bahou, Cuogang and Yakeshi stations (Duan et al. 2010). The severe drought occurred in 2001 (<1 SD) from the spring through the autumn (April, June–November), had caused a series of severe problems in most of northeastern China, including our study area. Large numbers of rivers and dams became dry, and grasslands degenerated as a result of the worse dry conditions (http://www.weather.com.cn/drought/ghsj/2001/05/443042.shtml). Spatial field displayed severe droughts in 1951 and 2007 extending to most part of Mongolia Plateau (Fig. 6), especially in central and eastern regions.

Prolonged dry or wet periods generally have strong effects on local or regional social and agricultural activities. Magnitude and intensity of two years or longer pluvial and droughts events were shown in Fig. 7. The six

**Table 3** Rank of years of extremely drought/wet reconstructed average April–August SPEI for the Hulun Buir steppe

Rank	Drought/year	Wet/year
1	−0.976/1907	0.942/1957
2	−0.809/1987	0.915/1868
3	−0.798/1951	0.709/1962
4	−0.786/2007	0.666/1958
5	−0.718/1856	0.619/1956
6	−0.682/2008	0.605/1959
7	−0.583/2003	0.485/1899
8	−0.578/1908	0.476/1888
9	−0.574/1920	0.472/1955
10	−0.546/1865	0.447/1862
11	−0.524/2004	0.404/1915
12	−0.520/1892	0.402/1984
13	−0.509/1905	0.397/1985
14	−0.464/2009	0.381/1898
15	−0.454/1906	0.377/1874
16	−0.454/1917	0.366/1948
17	−0.441/1909	0.349/1991
18	−0.441/1926	0.348/1963
19	−0.428/1936	0.348/1980
20	−0.423/2001	0.341/1953
21	−0.416/1969	0.336/1949
22	−0.358/1927	0.333/1934
23		0.333/1945

most significant droughts and pluvial spans in our reconstruction, lasting 5 years or more, were listed (Table S1). The longest duration drought belongs to 2000–2009 with the greatest magnitude of −4.307, but the second one in 1904–1910 owns the strongest intensity of −0.47. The pluvial interval in 1952–1960 exhibits the strongest magnitude (4.336) and intensity (0.482). The intensity (–0.644) of extremely dry event in 2007–2009 (<1 SD) is higher than that (−0.592) in 1905–1909 (<1 SD), even though the magnitude (−1.932) is smaller than latter (−2.958) (Fig. 7d, b). This result may suggest that dry event intensity could be enhanced if regional temperature continues increasing, while precipitation keeps slightly decreasing in future (Fig. 2c, d). Severe drought-stress in 2007–2009 leading to tree mortality at many lower elevation xeric forest-grassland ecotones and vicinity in Inner Asia has been observed (Liu et al. 2013).

4.3 Regional comparison and potential climate regimes

Our average April–August SPEI (RECSPEI48) reconstruction was significantly correlated with the same period climate factors, including temperature (Fig. 8a) and precipitation (Fig. 8b). A larger area was covered by

Fig. 6 The area of the severe drought anomaly of June–August SPEI04 for 1951 (<2 SD) (*top*) and 2007 (<2 SD) (*bottom*)
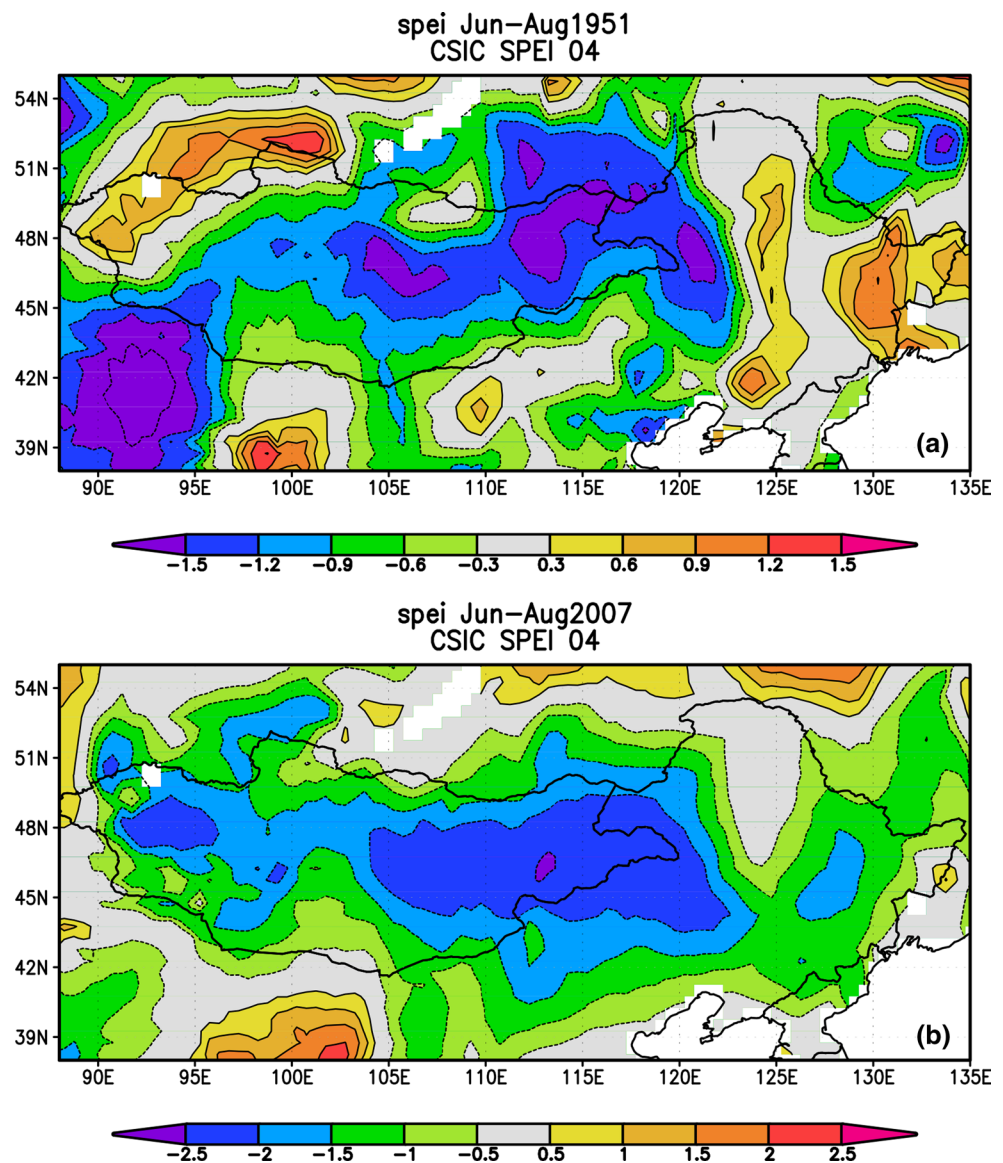

the significant correlation with SPEI03 field in central and eastern Mongolian Plateau (Fig. 8c). The areas represented by the Selenge (Davi et al. 2006) and Kherlen (Pederson et al. 2001) streamflow reconstructions were also overwhelmed by the RECSPEI48 reconstruction (Fig. 8d, e). Spatial correlation of the Yeruu reconstruction and Selenge reconstruction with June–August averaged precipitation from CRU TS3.1 spanning 1950–2001 (see Fig. 5 in Pederson et al. 2013) also confirmed that our reconstruction contains regional-scale moisture signal in central and eastern Mongolian Plateau and vicinity. This pattern was consistent with the region identified by the first EOF modes which were performed on the annual precipitations in the period from 1960 to 2009 over the entire mid-latitude Asia (see Figs. 1 and 2 in Huang et al. 2013).

Three sources are available to examine the hydroclimatic variations in this large area through time. One dataset is a tree-ring based reconstruction of the April–October streamflow of the Selenge River in west-central Mongolia, a location approximately 1,300 km west of our study area (Davi et al. 2006). The second dataset, from a location approximately 1,000 km northwest of our study area, is a reconstruction of the May–September streamflow of the Yeruu River, based on tree rings in northern Mongolia (Pederson et al. 2013). The third dataset, from a location approximately 800 km southwest of our study area, is the first principal component index of tree-ring chronologies (PC1 index) which was used to reconstruct the August–July streamflow of the Kherlen River in northeastern Mongolia (Pederson et al. 2001). Synchronous changing patterns existed in our RECSPEI48 reconstruction,

Fig. 7 Temporal distribution of **a** magnitude and **c** intensity of pluvial and drought events two-year or more in duration for the reconstructed average April–August SPEI, **b** magnitude and **d** intensity for the reconstructed extreme wet (>1 SD at least) and dry years (<1 SD). Magnitude represents the cumulative severity of each event whereas the intensity indicates the average severity of each event
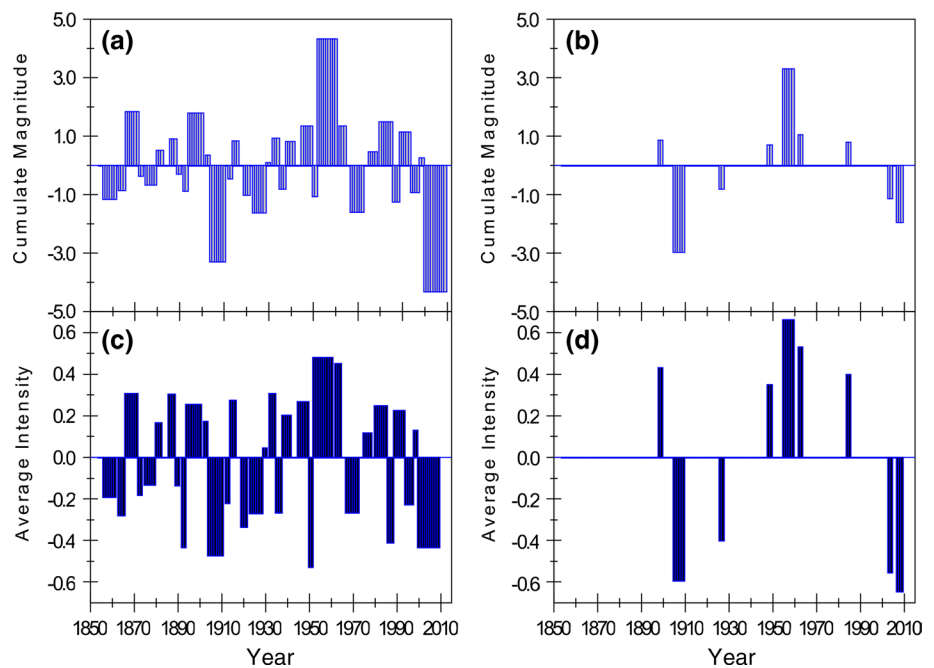
the Selenge and Yeruu River reconstruction, as well as the PC1 index, with different degrees of bidecadal-scale variations present through time (Fig. 9). Roughly, all the four series shown pluvial intervals in the late 1860s-early 1870s, 1890s, 1910s, 1930s, the late 1950s-early 1960s and the late 1980s-early 1990s, implying that these events were regional-scale or extra-basin-scale events (Davi et al. 2013). The wettest five-year event in 1955–1959 inferred from the drought reconstruction for Mongolia based on a large-scale tree ring network from 1520 to 1993 (Davi et al. 2010) coincided with the longest pluvial interval in 1952–1960 of our RECSPEI48 series (Table S1). This significant pluvial consistent with the most moisture period of 1948–1965 in the PDSI reconstruction and of 1956–1958 in summer precipitation index for the Ortindag Sand Land, east Inner Mongolia (Liang et al. 2007) and north-central China since 1470 AD based on drought/flood index and tree-ring records (Yi et al. 2012), respectively. Droughts appeared in the late 1850s–early 1860s, the late 1870s-early 1880s, 1900s, 1920s, 1970s and since the late 1990s implied the spatial expression of hydroclimatic signal were captured at regional scales in central and eastern Mongolian Plateau (Davi et al. 2013). The driest five-year event in 1854–1858 inferred from the Selenge River reconstruction (Davi et al. 2006) and severe drought in 1858–1866 of the east Inner Mongolia PDSI reconstruction (Liang et al. 2007) agreed with the severe drought in 1856–1861 obtained from our RECSPEI48 (Table S1). The common variations displayed in these reconstructions based on the moisture-sensitive growth of trees in such a large area could reveal a possible linkage between the regional-scale drought variability

in central and eastern Mongolia Plateau and large-scale climate forcing.

Spectral analysis indicated that the average April–August SPEI (RECSPEI48) reconstruction exhibits variability at inter-annual to multi-decadal time-scales. Significant cycles were found for periods of 7.38 ($p < 0.1$), 8.61 ($p < 0.05$), 15.5 ($p < 0.01$), 19.37 ($p < 0.01$), 31 ($p < 0.01$), and 77.5 ($p < 0.01$) years (Fig. 10). The significant peak of 7.38 year falls within range of El Niño-Southern Oscillation (ENSO) variability (Allan et al. 1996; Sun and Wang 2007). The effects of ENSO on the strength of Asian summer monsoon, then resulting in precipitation changes in northern China and the marginal monsoon areas such as our study region have been documented (Lu 2005; Zhang et al. 1999). Significant negative correlations of our reconstruction with the ENSO-related sea surface temperature (SST) confirmed this teleconnection between drought variability in central and eastern Mongolian Plateau and vicinity and remote oceans (Fig. S1). When SST in the eastern equatorial Pacific Ocean increases during ENSO warm phase, the descending arm of the Hadley circulation will be intensified, then induces a stronger western Pacific subtropical high. Along with a westward shift of the location of the subtropical high, the Indian summer monsoon tends to decrease the influence on the northerly extent. This results in precipitation reducing in the semi-arid region of north China (Fu and Li 1978; Li et al. 1979).

The severe drought occurred in the late 1870s–early 1880s (Fig. 9) likely corresponds to the failure of the Indian summer monsoon during one of the strongest El Niño events in 1876–1878 during the past 150 years (Cook
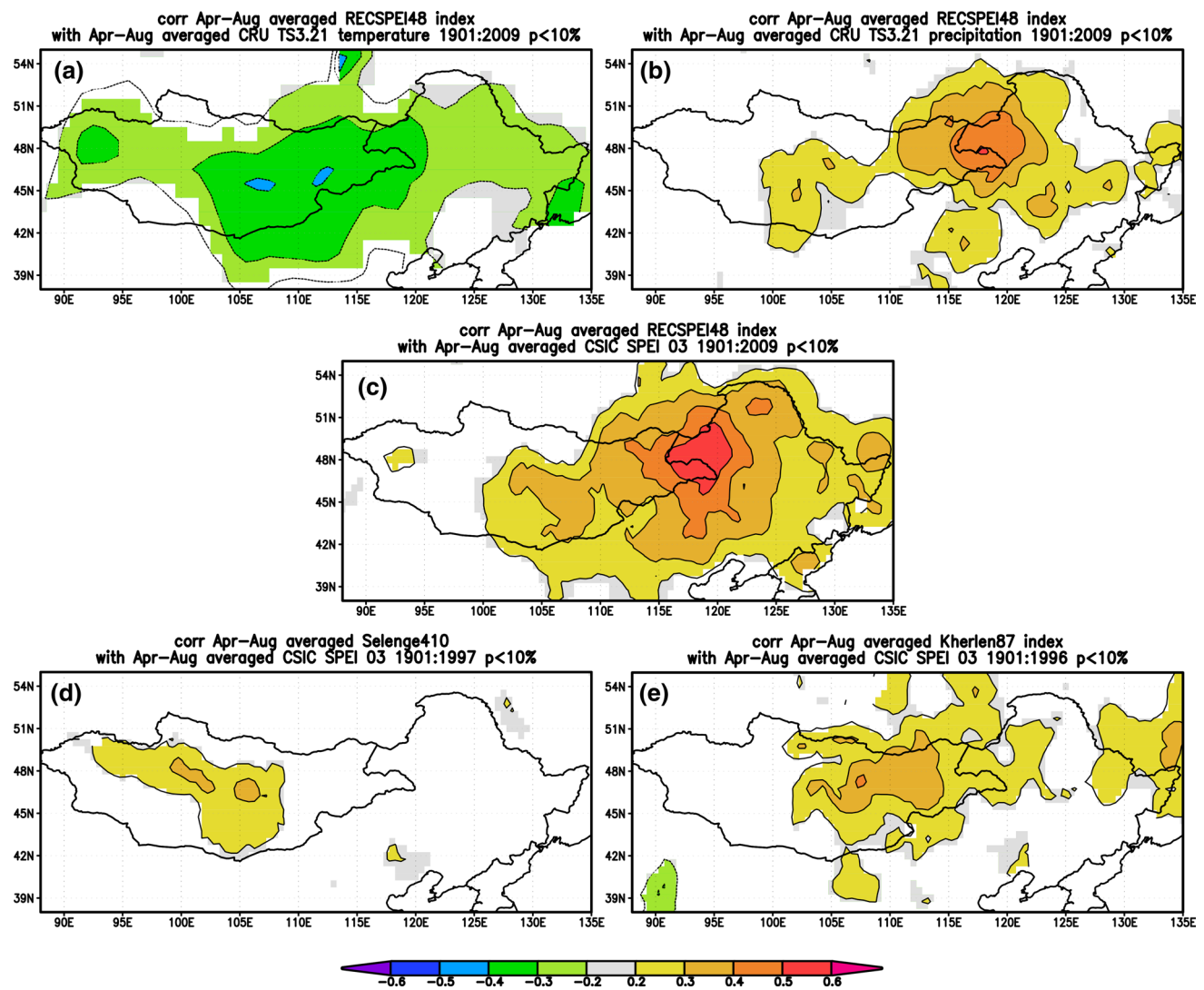
Fig. 8 Spatial correlation patterns of reconstructed average April–August SPEI with **a** mean temperature and **b** total precipitation of April–August SPEI with CRU TS3.1 grid dataset during 1901–2009 (Mitchell and Jones 2005), **c** the average April–August SPEI03 dataset during 1901–2009 (Vicente-Serrano et al. 2010b). Spatial correla-tions between the reconstructions of **d** the Selenge River (Davi et al. 2006) and **e** the Kherlen River streamflow (Pederson et al. 2001) with the average April–August SPEI03 dataset (Vicente-Serrano et al. 2010b) during 1901–1997 and 1901–1995, respectively

et al. 2010; Davis 2001; Feng et al. 2013; Zhang and Liang 2010). Not only the entirety of India and a majority of Pakistan suffered from severe precipitation deficit, but also the regions of northern China and nearby where it was esti-mated about 20–30 % precipitation deficit occurred during that drought (see Fig. 5d in Feng et al. 2013).

Strong negative correlations with SST was very clear for the western Pacific Warm Pool region over the Philippines, the South China Sea and Indian Ocean (Fig. 11), indicat-ing that effects on climate and tree growth in our study area that involve more than just ENSO. The similar climate-growth responses have been found in Thailand (Buckley et al. 2007) and Vietnam (Sano et al. 2009), Southeast Asia. When the Indian Ocean and the eastern Pacific sea surface

temperature was low, the West Pacific subtropical high shrank and retreated northeastward. In this situation, mon-soonal China is mainly dominated by the tropical monsoon trough, i.e. the Intertropical Convergence Zone (ITCZ) (Tan 2009), more moisture flux from the Indian Ocean could lead to enhancing rainfall in the Chinese monsoon zone. Positive correlations between RECSPEI48 and April–August rainfall of the whole Indian, eastern and western peninsula from 1953 to 2006 are 0.247 ($p = 0.072$), 0.283 ($p = 0.038$) and 0.365 ($p = 0.007$), respectively (Sontakke et al. 2008), which indicated that moisture convergence in central and eastern Mongolian Plateau was consistent with atmospheric moisture originating from the Indian monsoon to some extent. Significantly positive correlation

Fig. 9 Comparison of **a** reconstructed average April–August SPEI in this study, **b** the Selenge River streamflow reconsruction (Davi et al. 2006), **c** the first principal component index of tree-ring chronologies (PC1 index) utilized to reconstruct the August–July streamflow of the Kherlen River in northeastern Mongolia (Pederson et al. 2001) and **d** the Yeruu River streamflow reconstruction (Pederson et al. 2013). The *bold line* represents the 20-year low pass data. The *red-shaded areas* represent severe drought intervals discussed in text
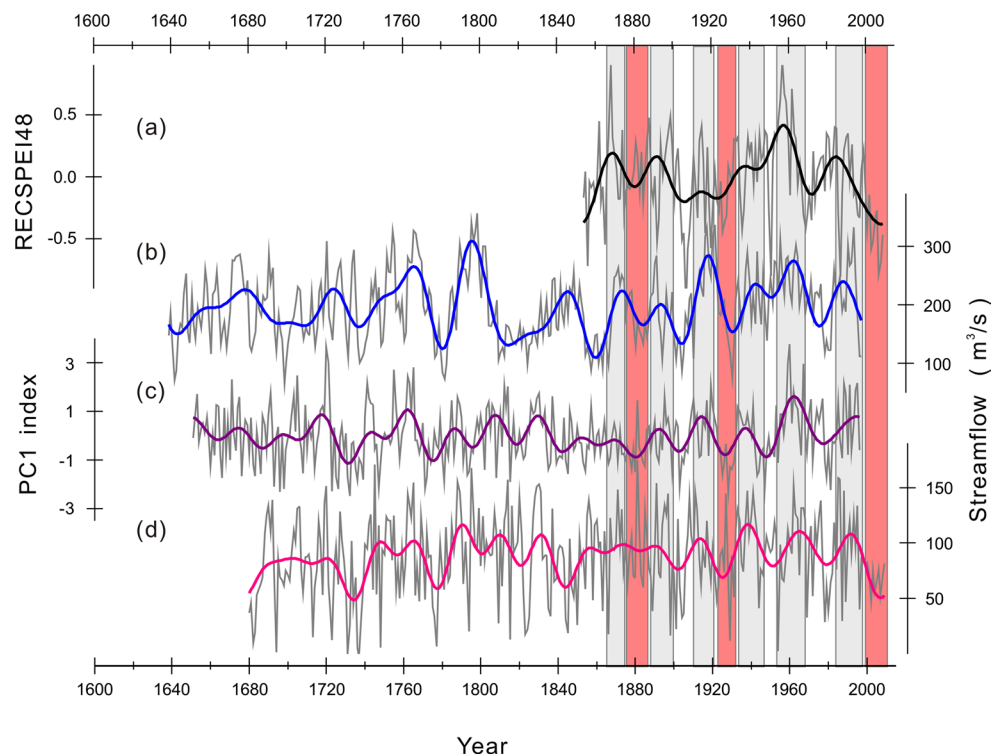
of precipitation associated with interannual variability of the monsoon in Indian and in northern China has been revealed in previous studies (Guo and Wang 1998; Kriplani and Kulkarni 2001). A similar result was revealed by the drought reconstruction tree-ring based in the monsoon marginal area, north central China (Kang et al. 2012). It should be noted that the moisture connection is not stable. Wang and Huang (2006) reported that the instability of the summer rainfall in northern China and Indian and attributed to the variations of the SST in eastern equatorial Pacific Ocean. In fact, when the Indian Ocean and the eastern Pacific sea surface temperature was high, then the West Pacific subtropical high enhanced and extended southwestward resulting in the moisture decreasing from the Indian Ocean (Tan 2009). The amount of change in moisture should be a factor for this unstable connection. Warm anomaly of tropical Indian Ocean may cause the anomalous of negative precipitation or convective activity near the Philippines, which plays an important role in forming the Pacific–Japan/East Asia–Pacific (PJ/EAP) patternlike wave train on the multidecadal time scale (Huang and Sun 1992; Hu et al. 2011), further results in deficient precipitation in northern China (Qian and Zhou 2014). Two possible mechanisms are involved: one is to create favorable anticyclone conditions over the Philippine Sea through Kelvin wave responses suppressing the convection forced by convective heating of the Indian Ocean (Wu et al. 2009), the other is to induce local Hadley circulation and cause anomalous subsidence near the Philippines through the increase of surface

moisture over the Indian Ocean and the advection strengthened convective heating over the Maritime Continent (Hu 1997).

Another severe drought in 1920s captured in our reconstruction (Fig. 9) was considered to be the most extreme over the pass 500 years based on the multi-proxy reconstruction of May–September precipitation over the Asian continent (Feng et al. 2013). The extent of its influence covered most part of China, Pakistan and Indian (see Fig. 5e in Feng et al. 2013). Only in northern China, more than 4 million people perished because of famines and diseases induced by the widespread droughts (Liang et al. 2006). The 1920s drought coincided with high temperature and low precipitation in Northwestern China (Liang et al. 2003, 2006), which was supported by Yi et al. (2012), who identified the drought types based on drought/flood index and tree-ring records since 1470 AD for north-central China. For instance, the droughts from 1926 to 1930 were totally or partly due to above average temperature (see Table 8 in Yi et al. 2012). Two multidecadal oscillations at ~20-year and ~70-year timescales were revealed from historical documents and instrumental records from China by signal analysis from wavelet transform (Qian et al. 2007, 2012), and the severe drought in 1927–1929 in northern China was a result of coinciding with the anomalous warm and dry decade, based on the two oscillations (Qian et al. 2007). The near-80-year oscillation was a dominating mode of the interdecadal variability of the summer precipitation in China, and other modes of 12–14, 18–20, 30–40 years

Fig. 10 Spectral (**a**) and wavelet (**b**) (Paul 4; Torrence and Compo 1998) analysis for reconstructed average April–August SPEI for the period 1854–2009. The 95 % confidence interval for peaks in the power spectrum is indicated by the *pink line*. The cone of influence in the wavelet analysis is indicated by the *black line*
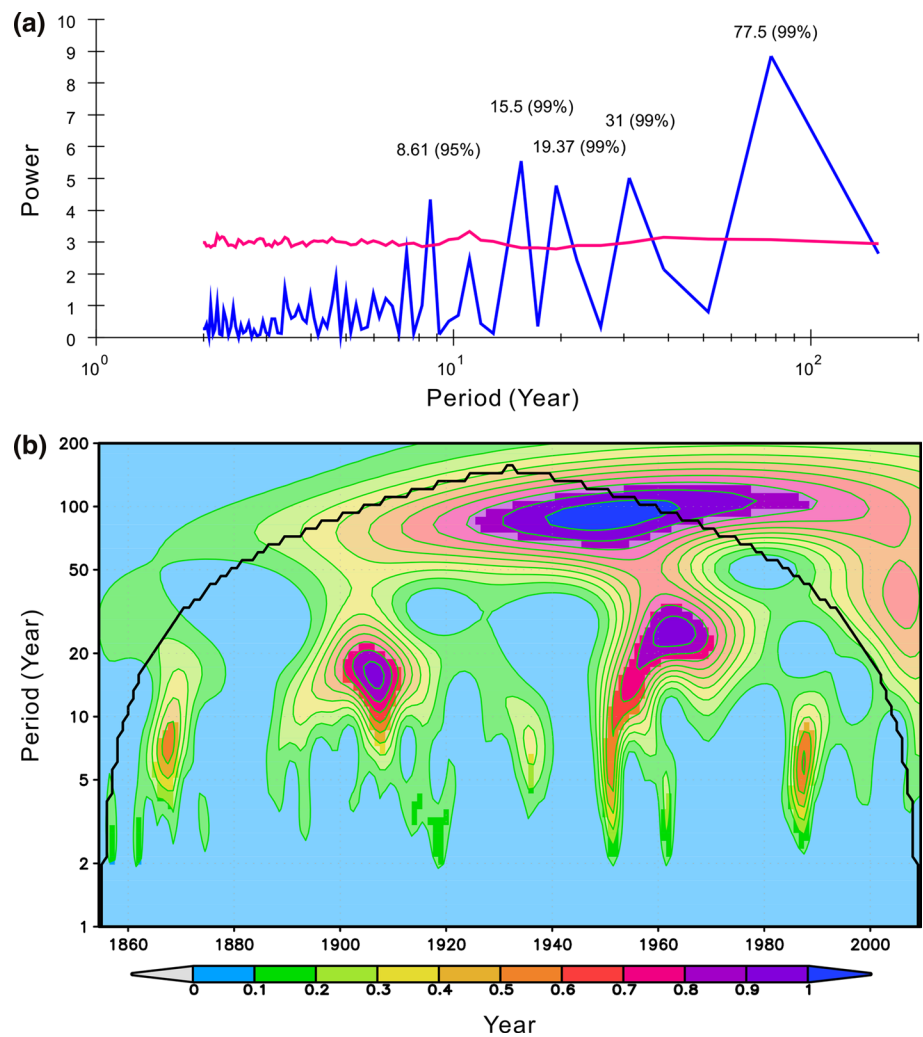
Fig. 11 Spatial correlation patterns of reconstructed average April–August SPEI with the sea surface temperature of NCDC ERSSTv3 (Smith et al. 2008) during the period 1953–2009
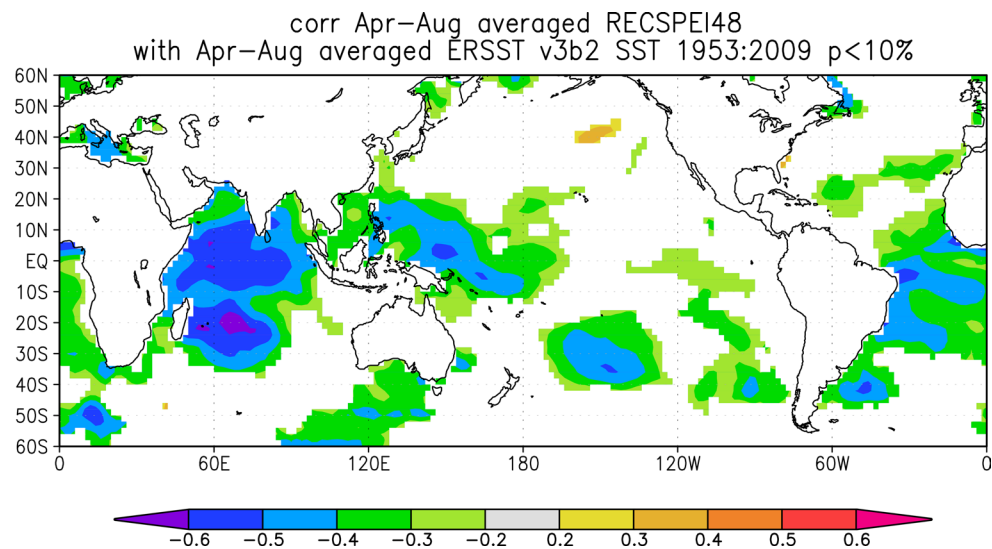
oscillations also played an important role in affecting regional inter-decadal variability (Ding et al. 2008). The similar oscillations were revealed from the reconstruction of Summer Sea Level Pressure (SLP) over East Asia from 1470 to 2008, which had a close relationship with the precipitation index in eastern China (Wei et al. 2012). In

particular, significant spectrum power at multidecadal variability of 60–90 years occurred since 1750 AD, which agreed with the span of our 77.5 years cycle appeared (Fig. 10). Therefore, the same drought mechanism could be inferred from the significant decadal variability at 19.37, 31 and 77.5 years in our RECSPEI48 reconstruction.

The Pacific Decadal Oscillation (PDO) exhibits considerable influence on summer precipitation in eastern China, by modulating the strength of the summer monsoon and the location of the subtropical high (Gong and He 2002; Gu et al. 2004). Dry periods in both North and South China and wet periods in the middle and lower Yangtze River Valley were consist with warm phases of the PDO, companying with the week summer monsoon and the strong subtropical high locating far to the south and west, and vice versa in cool phases. That means the warm phase PDO in 1920s–1940s could be a contributor to the drought in 1920s, as well as the very strong El Niño episodes in 1925 and 1926 (Quinn and Neal 1992) which falling within the third longest dry duration of 1923–1928 appeared in RECSPEI48 (Table S1). The relationship between drought and the PDO is confirmed by the significantly negative correlation of the Palmer drought severity index (PDSI) in north China with the PDO index during 1900–2010, particularly at the 50–70-year timescale (Qian and Zhou 2014). They suggest that an anomalous PJ/EAP patternlike wave train revealed from composite differences of two positive PDO phases (1922–1945 and 1977–2002) and one negative PDO phase (1946–1976) for summertime may locally respond to the PDO-related warm sea surface temperature anomalies in the tropical Indo-Pacific Ocean and extends from the tropical western Pacific to north China along the East Asian coast. Under the positive PDO phase, north China is dominated by an anomalous high pressure and anticyclone system in the mid-lower troposphere, which are favorable for dry conditions. Krishnamurthy and Krishnamurthy (2013) has proposed a hypothesis to illustrate the mechanism by which PDO could affect the South Asian monsoon rainfall through the seasonal footprinting of SST (Vimont et al. 2001, 2003) from the North Pacific to the subtropical Pacific and further through the Walker and Hadley circulations. This mechanism could support the results mentioned above of Qian and Zhou (2014) and confirm the drought of northern China associated with the PDO. Significant correlation ($r = -0.275$, $p = 0.007$, n = 95 for 1900–1994) existed in first-difference series of RECSPEI48 and the PDO reconstruction index (Felis et al. 2010) and their 21-year sliding correlation agreed well with the pattern of Qian and Zhou (2014, see Fig. 4b) (Fig. S2).

The latest drought since late 1990s to present was consistent with the weakening of the East Asian summer monsoon since the end of 1970s (Cook et al. 2010; Wang 2001; Zhang et al. 2008), further resulting in much deficient moisture supply for precipitation in North China (Ding et al. 2008) and in our study area and vicinity (Huang et al. 2013). Along with the higher mean SST in equatorial eastern Pacific in 1978–2000, the influence of ENSO on the East Asian summer circulation experienced a significant strengthening after the late 1970s (Ding et al. 2010). Similar effects of the warm phase PDO since late 1970s on the decreasing moisture conditions in North China and nearby had been identified by Ma (2007). It should be noted that the latest drought since late 1990s in our RECSPEI48 reconstruction might not be the driest event in a long perspective of the moisture variations for Mongolia, reflected by the Yeruu River streamflow (Pederson et al. 2013) and a new Kelunlun River streamflow reconstruction (not shown) (Davi et al. 2013) (Fig. 9). In fact, compared with the SPEI, rivers covering larger draining areas could integrate precipitation, evaporation, topography, lithology and vegetation heterogeneities thus represent regional-scale climatic fluctuations (Labat 2006; Probst and Tardy 1987). Hence, it is credible that the recent drought might be a return to more characteristic hydroclimatic conditions over the past several centuries in the Mongolian Plateau (Davi et al. 2013; Pederson et al. 2013).

In addition, intermittent multiannual and interdecadal patterns of variability existed in the land-surface hydrological cycles were consistent with known sea surface temperature and pressure fluctuations, such as the ENSO, PDO and North Atlantic Oscillation (NAO) (Labat 2006). The Atlantic Multidecadal Oscillation (AMO) could be suggested a pacemaker of Northern Hemisphere surface temperature (Zhang and Delworth 2007) and global air temperature (Kravtsov and Spannagle 2008). The influence of the AMO on Asian monsoonal climate has received much attention. For instance, Li and Bates (2007) found that the warm-phase AMO favors warmer winters in much of China, while more precipitation is induced in northern China based on the observational analyses and numerical simulations using atmospheric general circulation models. Wang et al. (2009) also revealed the warm-phase AMO tends to enhance air temperatures in East Asia and northern India, and causes more rainfall in central and southern India, particularly in summer and fall. The possible mechanism was suggested that through warming Eurasian middle and upper troposphere in all four seasons, resulting in weakened Asian winter monsoons but enhanced summer monsoons. Significant correlation of RECSPEI48 with tree-ring based reconstruction of North Atlantic sea surface temperature anomalies ($r = 0.211$, $p = 0.013$, n = 137 for 1854–1990) (Gray et al. 2004) may suggest the connection between our study area and the North Atlantic, though the mechanism still needs to be explored. Recently, teleconnection between the summer North Atlantic Oscillation (SNAO) and the East Asian summer monsoon had been confirmed (Linderholm et al.

2011) and the strongest SNAO-tree ring width associations were found in central East Asia (Mongolia and nearby) and the eastern Tibetan Plateau (Linderholm et al. 2013). The connection between the SNAO and the East Asian summer precipitation on decadal timescale is enhanced after the late 1970s (Sun and Wang 2012). With its southern center shifting eastward since then, the SNAO pattern has changed the zonal wave activity over the Eurasian Continent, leading to a meridional dipole pattern over East Asia. This dipole pattern strongly influences on the dynamical and moisture conditions over East Asia, including divergence circulation, vertical motion, water vapor condition, and total cloud cover, which produces the reverse summer precipitation variability over central and northern East Asia. In a positive-phase SNAO year, more summer precipitation occurs in central East Asia, but less precipitation appears in northern East Asia, and vice versa. At the same time, associated with the centers of the SNAO pattern locating more eastward, a strong linkage of the SNAO and simultaneous East Asian air temperature on decadal timescale also appears after the late 1970s (Sun et al. 2008). A positive-phase (negative-phase) SNAO favors a cool (warm) summer over central East Asia. The possible mechanism attributes to that a positive-phase (negative-phase) SNAO stimulates a strong upper-level convergence (divergence) via the Ekman pumping after producing a strong lower-level divergence (convergence) over the Asian jet entrance region (Mediterranean Sea), by which a zonally oriented quasi-stationary barotropical Rossby wave train along the Asian upper-level jet is excited, then the SNAO signal is transported eastward to East Asia, resulting in an anomalous summer air temperature over that region. In summary, moisture/cool (dry/warm) conditions consist with positive-phase (negative-phase) SNAO years in central East Asia. Extreme years of wet (1985, 1991) and dry (1987, 2001) of our reconstruction agree with that pattern (Table 3).

For the position locating in the center of Asia, the Mongolian Plateau is mainly controlled by an extreme continental climate. In winter, the plateau is dominated by the Siberian High, which closely relates to the NAO and NPO (North Pacific Oscillation) (Gong et al. 2001; Hoerling et al. 2001; Kerr 1999). Another two large-scale climate systems play important roles in the climate and environment of the Mongolian Plateau. The first system consists of the westerlies modulated by the North Atlantic (Visbeck 2002), and the second system is the East Asian summer monsoon, which associates with the ENSO and the ITCZ (the Inter-tropical Convergence Zone) (Tudhope et al. 2001). Recently, Indian Ocean has been found to be the predominant moisture source of the East Asia Summer Monsoon (EASM), which suggests precipitation change associated with the EASM in northern China (including our study area and nearby) could be connected to the coherent continental scale variability of the Asian monsoon in the upstream Indian Ocean region (Liu et al. 2014). Trees growing on the Mongolian Plateau and its vicinity could record information on climatic variations influenced by large-scale climate forcing. Our April–August SPEI reconstruction for the Hulun Buir steppe represents moisture variations in eastern Mongolian Plateau to some extent. To better understand the physical mechanisms behind the relationships represented by teleconnections, more dendroclimatological studies should be conducted in the future, especially in the region where meteorological records are typically sparse and spatially diffuse, just like the Mongolian Plateau.

5 Conclusions

The average April–August standardized precipitation evapotranspiration index (SPEI) has been reconstructed using a robust regional *Pinus sylvestris* var. *mongolica* tree-ring chronology developed for the Hulun Buir region, Inner Mongolia, a border area in the eastern Mongolian Plateau. Similar fluctuation patterns of drought and pluvial intervals existed in several available tree-ring-based hydroclimatic reconstructions and ours. The recent drought events from late 1990 to present are not unusual in the context of the past several centuries according to the region comparation. Significant cycle results and correlations between the reconstruction and indices of PDO, AMO and SST suggest the influences of large-scale climate forcing variability on drought variations in eastern Mongolian Plateau. The present study is the first to demonstrate the potential of using *Pinus sylvestris* var. *mongolica* tree-ring data to reconstruct SPEI variability for the eastern Mongolian Plateau. More comprehensive tree-ring networks should be developed, including additional tree-ring parameters (i.e. stable isotopes), to better understand the spatial and temporal variability of past drought changes over such a large climate-sensitive area.

References

Allan RJ, Lindesay JA, Parker DE (1996) El Niño Southern Oscillation and climatic variability. CSIRO Publishing, Australia

Bao G, Liu Y, Linderholm HW (2012) April–September mean maximum temperature inferred from Hailar pine (Pinus sylvestris var. mongolica) tree rings in the Hulunbuir region, Inner Mongolia, back to 1868 AD. Palaeogeogr Palaeoclimatol Palaeoecol 313–14:162–172

Batima P (2006) Potential impacts of climate change and vulnerability and adaptation assessment for grassland ecosystem and livestock sector in Mongolia. Final Report: observed climate change in Mongolia, AIACC. Project AS06, Institute of Meteorology and Hydrology, Ulaanbaatar, Mongolia

Biondi F, Kozubowski TJ, Panorska AK (2002) Stochastic modeling of regime shifts. Clim Res 23:23–30

Buckley BM, Palakit K, Duangsathaporn K, Sanguantham P, Prasomsin P (2007) Decadal scale droughts over northwestern Thailand over the past 448 years: links to the tropical Pacific and Indian Ocean sectors. Clim Dyn 29:63–71

Cai QF, Liu Y, Bao G, Lei Y, Sun B (2010) Tree-ring-based May–July mean temperature history for Lüliang Mountains, China, since 1836. Chin Sci Bull 55:3008–3014

Chen ZJ, Zhang XL, Cui MX, He XY, Ding WH, Peng JJ (2012) Tree-ring based precipitation reconstruction for the forest-steppe ecotone in northern Inner Mongolia, China and its linkages to the Pacific Ocean variability. Glob Planet Change 86–87:45–56

Chinese Academy of Sciences (Compilatory Commission of Physical Geography of China) (1984) Physical Geography of China: climate. Science Press, Beijing (in Chinese)

Cook ER (1985) A time series analysis approach to tree ring standardization. PhD. The University of Arizona, Tucson

Cook E, Kairiukstis L (1990) Methods of dendrochronology: applications in the environmental science. Kluwer, Dordrecht

Cook ER, Briffa KR, Jones PD (1994) Spatial regression methods in dendroclimatology: a review and comparison of two techniques. Int J Climatol 14:379–402

Cook ER, Meko DM, Stahle DW, Cleaveland MK (1999) Drought reconstructions for the Continental United States. J Clim 12:1145–1162

Cook ER, Woodhouse CA, Eakin CM, Meko DM, Stahle DW (2004) Long-term aridity changes in the western United States. Science 306:1015–1018

Cook ER, Anchukaitis KJ, Buckley BM, D'Arrigo RD, Jacoby GC, Wright WE (2010) Asian monsoon failure and megadrought during the last millennium. Science 328:486–489

Dai AG (2011) Drought under global warming: a review. Wiley Interdiscip Rev Clim Chang 2:45–65. doi:10.1002/wcc.81

Dai AG, Trenberth KE, Qian T (2004) A global dataset of palmer drought severity index for 1870–2002: relationship with soil moisture and effects of surface warming. J Hydrometeorol 5:1117–1130

D'Arrigo R, Jacoby G, Pederson N, Frank D, Buckley B, Nachin B, Mijiddorj R, Dugarjav C (2000) Mongolian tree-rings, temperature sensitivity and reconstructions of Northern Hemisphere temperature. Holocene 10:669–672

D'Arrigo R, Jacoby G, Frank D, Pederson N, Cook E, Buckley B, Nachin B, Mijiddorj R, Dugarjav C (2001) 1738 years of Mongolian temperature variability inferred from a tree-ring width chronology of Siberian pine. Geophys Res Lett 28:543–546

Davi NK, Jacoby GC, Curtis AE, Baatarbileg N (2006) Extension of drought records for central Asia using tree rings: West-central Mongolia. J Clim 19:288–299

Davi N, Jacoby G, D'Arrigo, Baatarbileg N, Li J, Curtis A (2009) A tree-ring based drought index reconstruction for far western Mongolia: 1565–2004. Int J Climatol 29:1508–1514

Davi N, Jacoby G, Fang K, Li J, D'Arrigo R, Baatarbileg N, Robinson D (2010) Reconstructing drought variability for Mongolia based on a large-scale tree ring network: 1520–1993. J Geophys Res 115:D22103. doi:10.1029/2010JD013907

Davi NK, Pederson N, Leland C, Nachin B, Suran B, Jacoby GC (2013) Is eastern Mongolia drying? A long-term perspective of a multidecadal trend. Water Resour Res 49:151–158

Davis M (2001) Late Victorian Holocausts: El Niño Famines and the Making of the Third World. Verso, pp 470

Ding YH, Wang ZY, Sun Y (2008) Inter-decadal variation of the summer precipitation in East China and its association with decreasing Asian summer monsoon. Part I: observed evidences. Int J Climatol 28:1139–1161

Ding RQ, Ha KJ, Li JP (2010) Interdecadal shift in the relationship between the East Asian summer monsoon and the tropical Indian Ocean. Clim Dyn 34:1059–1071

Duan LM, Liu TX, Wang XX, Luo YY, Wu L (2010) Development of a regional regression model for estimating annual runoff in the Hailar River Basin of China. J Water Resour Protec 2:934–943

Fang K, Gou X, Chen F, Frank D, Liu C, Li J, Kazmer M (2012) Precipitation variability during the past 400 years in the Xiaolong Mountain (central China) inferred from tree rings. Clim Dyn 39:1697–1707

Felis T, Suzuki A, Kuhnert H, Rimbu N, Kawahata H (2010) Pacific decadal oscillation documented in a coral record of North Pacific winter temperature since 1873. Geophys Res Lett 37:L14605. doi:10.1029/2010GL043572

Feng S, Hu Q, Wu Q, Mann ME (2013) A gridded reconstruction of warm season precipitation for Asia spanning the past half millennium. J Clim 26:2192–2204

Fritts HC (1976) Tree rings and climate. Academic Press, New York

Fu C, Li K (1978) The effects of tropical ocean on the western Pacific subtropical high. Oceanic Selections, No. 2. Ocean Press, Beijing, pp 16–21

Fu CB, Wei HL, Chen M, Su BK, Zhao M, Zhen WZ (1998) Evolution of summer monsoon rain belts over East China in a regional climate model. Chin J Atmos Sci 22:522–534

Gong D, He X (2002) Interdacadal change in western Pacific subtropical high and climatic effects. Acta Geogr Sinica 57:185–193

Gong DY, Wang SW, Zhu JH (2001) East Asian winter monsoon and arctic oscillation. Geophys Res Lett 28:2073–2076

Gray ST, Graumlich LJ, Betancourt JL, Pederson GT (2004) A tree-ring based reconstruction of the Atlantic multidecadal oscillation since 1567 AD. Geophys Res Lett 31:L12205

Gray ST, Lukas JJ, Woodhouse CA (2011) Millennial-length records of streamflow from three major upper Colorado River Tributaries. J Am Water Resour Assoc 47:702–712

Gu Q, Cai J, Shao X, Sha W (2004) Studies on the variations of east Asian summer monsoon during A.D. 1873–2000. Chin J Atmos Sci 28:206–215

Guo Q, Wang J (1998) A comparison of the summer precipitation in India with that in China (in Chinese). J Trop Meteorol 4:53–60

He JC, Wang LL, Shao XM (2005) The relationships between Scots pine tree ring indices and normalized difference vegetation index in Mohe, China (in Chinese). Quat Sci 25:252–257

Hoerling MP, Hurrell JW, Xu T (2001) Tropical origins for recent North Atlantic climate change. Science 292:90–92

Holmes RL (1983) Computer-assisted quality control in tree-ring dating and measurement. Tree Ring Bull 43:69–78

Hu Z (1997) Interdecadal variability of summer climate over East Asia and its association with 500-hPa height and global sea surface temperature. J Geophys Res 102(D16):19403–19412

Hu K, Huang G, Huang R (2011) The impact of tropical Indian Ocean variability on summer surface air temperature in China. J Clim 24:5365–5377

Huang RH, Sun FY (1992) Impacts of the tropical western Pacific on the East Asian summer monsoon. J Meteor Soc Japan 70:243–256

Huang W, Chen FH, Feng S, Chen JH, Zhang XJ (2013) Interannual precipitation variations in the mid-latitude Asia and their

association with large-scale atmospheric circulation. Chin Sci Bull. doi:10.1007/s11434-013-5970-4

Kang SY, Yang B, Qin C (2012) Recent tree-growth reduction in north central China as a combined result of a weakened monsoon and atmospheric oscillations. Clim Chang 115:519–536

Kerr RA (1999) A new force in high-latitude climate. Science 284:241–242

Kravtsov SV, Spannagle C (2008) Multi-decadal climate variability in observed and modeled surface temperatures. J Clim 21:1104–1121. doi:10.1175/2007JCLI1874.1

Kriplani RH, Kulkarni A (2001) Monsoon rainfall variations and teleconnections over south and east Asia. Int J Climatol 21:603–616

Krishnamurthy L, Krishnamurthy V (2013) Influence of PDO on South Asian monsoon and monsoon-ENSO relation. Clim Dyn. doi:10.1007/s00382-013-1856-z

Labat D (2006) Oscillations in land surface hydrological cycle. Earth Planet Sci Lett 242:143–154

Li S, Bates GT (2007) Influence of the Atlantic multidecadal oscillation on the winter climate of East China. Adv Atmos Sci 24:126–135. doi:10.1007/s00376-007-0126-6

Li KR, Chen YS, Liu JF, Lan RH (1979) Some facts about the effect of the meridional difference of SST anomalies of north Pacific on the subtropical high. Sci Atmos Sin 3:150–157

Liang E, Shao X, Kong Z, Lin J (2003) The extreme drought in the 1920s and its effect on tree growth deduced from tree ring analysis: a case study in North China. Ann For Sci 60:145–152

Liang E, Liu X, Yuan Y, Qin N, Fang X, Huang L, Zhu H, Wang L, Shao X (2006) The 1920s drought reconstructed by tree rings and historical documents in the semi-arid and arid areas of northern China. Clim Chang 79:403–432

Liang EY, Shao XM, Liu HY, Eckstein D (2007) Tree-ring based PDSI reconstruction since AD 1842 in the Ortindag Sand Land, east Inner Mongolia. Chin Sci Bull 52:2715–2721

Liang EY, Eckstein D, Shao X (2009) Seasonal cambial activity of relict Chinese pine at the northern limit of its natural distribution in north china—exploratory results. IAWA J 30:371–378

Linderholm HW, Ou TH, Jeong JH, Folland CK, Gong DY, Liu HB, Liu Y, Chen DL (2011) Interannual teleconnections between the summer North Atlantic Oscillation and the East Asian summer monsoon. J Geophys Res 116:D13107. doi:10.1029/2010JD015235

Linderholm HW, Seima A, Ou TH, Jeong JH, Liu Y, Wang XC, Bao G, Folland C (2013) Exploring teleconnections between the summer NAO (SNAO) and climate in East Asia over the last four centuries—a tree-ring perspective. Dendrochronologia. doi:10.1016/j.dendro.2012.08.004

Liu Y, Bao G, Song HM, Cai QF, Sun JY (2009) Precipitation reconstruction from Hailar pine (Pinus sylvestris var. mongolica) tree rings in the Hailar region, Inner Mongolia, China back to 1865 AD. Palaeogeogr Palaeoclimatol Palaeoecol 282:81–87

Liu HY, Williams AP, Allen CD, Guo DL, Wu XC, Anenkhonov OA, Liang EY, Sandanov DV, Yi NY, Qi ZH, Badmaeva NK (2013) Rapid warming accelerates tree growth decline in semi-arid forests of Inner Asia. Global Change Bio 19:2500–2510

Liu ZY, Wen XY, Brady EC, Otto-Bliesner B, Yu G, Lu HY, Cheng H, Wang YJ, Zheng WP, Ding YH, Edwards RL, Cheng J, Liu W, Yang H (2014) Chinese cave records and the East Asia Summer Monsoon. Quat Sci Rev 83:115–128

Lu R (2005) Interannual variation of North China rainfall in rainy season and SSTs in the quatorial eastern Pacific. Chin Sci Bull 50:2069–2073

Ma ZG (2007) The interdecadal trend and shift of dry/wet over the central part of North China and their relationship to the Pacific Decadal Oscillation (PDO). Chin Sci Bull 52:2130–2139

Meko DM, Graybill DA (1995) Tree-ring reconstruction of upper Gila River discharge. Water Resour Bull 31:605–616

Mitchell TD, Jones PD (2005) An improved method of constructing a database of monthly climate observations and associated high resolution grids. Int J Climatol 25:693–712

Osborn TJ, Briffa KB, Jones PD (1997) Adjusting variance for sample size in tree-ring chronologies and other regional mean time-series. Dendrochronologia 15:89–99

Pederson N, Jacoby GC, D'Arrigo RD, Cook ER, Buckley BM, Dugarjav C, Mijiddorj R (2001) Hydrometeorological reconstructions for Northeastern Mongolia derived from tree rings: AD 1651–1995. J Clim 14:872–881

Pederson N, Lealand C, Nachin B, Hessl AE, Bell AR, Martin-Benito D, Saladyga T, Suran B, Brown PM, Davi N (2013) Three centuries of shifting hydroclimatic regimes across the Mongolian Breadbasket. Agric For Meteor 178–179:10–20

Probst JL, Tardy Y (1987) Long range streamflow and world continental runoff fluctuations since the beginning of this century. J Hydrol 94:289–311

Qian C, Zhou TJ (2014) Multidecadal variability of North China aridity and its relationship to PDO during 1900–2010. J Clim 27:1210–1222

Qian WH, Lin X, Zhu YF, Xu Y, Fu JL (2007) Climatic regime shift and decadal anomalous events in China. Clim Chang 84:167–189

Qian W, Shan X, Chen D, Zhu C, Zhu Y (2012) Droughts near the northern fringe of the East Asian summer monsoon in China during 1740–2003. Clim Chang 110:373–383

Quinn WH, Neal VT (1992) The historical record of El Nino events. In: Bradley RS, Jones PD (eds) Climate since 1500 AD. Routledge, London, pp 623–648

Sano M, Buckley BM, Sweda T (2009) Tree-ring based hydroclimate reconstruction over northern Vietnam from Fokienia hodginsii: eighteenth century mega-drought and tropical Pacific influence. Clim Dyn 33:331–340

Shen JG (2008) Meteorological disasters dictionary of China: vol. Inner Mongolia. Eteorological Press, Beijing (in Chinese)

Smith TM, Reynolds RW, Peterson TC, Lawrimore J (2008) Improvements to NOAA's historical merged land-ocean surface temperature analysis (1880–2006). J Clim 21:2283–2296

Song H, Liu Y (2011) PDSI variations at Kongtong Mountain, China, inferred from a 283-year Pinus tabulaeformis ring width chronology. J Geophys Res 116:D22111. doi:10.1029/2011JD016220

Sontakke NA, Nityanand Singh, Singh HN (2008) Instrumental period rainfall series of the Indian region (1813–2005): revised reconstruction, update and analysis. Holocene 18:1055–1066

Sun M, Wang H (2007) Relationship and its instability of ENSO—Chinese variations in droughts and wet spells. Sci China, Ser D Earth Sci 50:145–152

Sun JQ, Wang HJ (2012) Changes of the connection between the summer North Atlantic Oscillation and the East Asian summer rainfall. J Geophys Res 117:D08110. doi:10.1029/2012JD017482

Sun JQ, Wang HJ, Yuan W (2008) Decadal variations of the relationship between the summer North Atlantic Oscillation and middle East Asian air temperature. J Geophys Res 113:D15107. doi:10.1029/2007JD009626

Tan M (2009) Circulation effect: climatic significance of the short term variability of the oxygen isotopes in stalagmites from monsoonal China—dialogue between paleoclimate records and modern climate research. Quat Sci 29:851–862

Torrence C, Compo GP (1998) A practical guide to wavelet analysis. Bull Am Meteorol Soc 79:61–78

Trenberth KE, Overpeck JT, Solomon S (2004) Exploring drought and its implications for the future. EOS Trans Am Geophys Union 85:27–29

Tudhope AW, Chilcott CP, McCulloch MT, Cook ER, Chappell J, Ellam RM, Lea DW, Lough JM, Shimmield GB (2001) Variability in the El Niño-Southern oscillation through a glacial-interglacial cycle. Science 291:1511–1517

Vicente-Serrano SM, Beguería S, López-Moreno JI (2010a) A multi-scalar drought index sensitive to global warming: the standardized precipitation evapotranspiration index-SPEI. J Clim 23:1696–1718

Vicente-Serrano SM, Beguería S, López-Moreno JI, Angulo M, Kenawy AE (2010b) A new global 0.5° gridded dataset (1901–2006) of a multiscalar drought index: comparison with current drought index datasets based on the Palmer Drought Severity Index. J Hydrometeorol 11:1033–1043

Vimont DJ, Battisti DS, Hirst AC (2001) Footprinting: a seasonal connection between the tropics and midlatitudes. Geophys Res Lett 28:3923–3926

Vimont DJ, Battisti DS, Hirst AC (2003) The seasonal footprinting mechanism in the CSIRO general circulation models. J Clim 16:2653–2667

Visbeck M (2002) The ocean's role in Atlantic climate variability. Science 297:2223–2224

Wang HJ (2001) The weakening of the Asian monsoon circulation after the end of 1970's. Adv Atmos Sci 18:376–386

Wang SW, Huang JB (2006) Instability of the teleconnection between the summer precipitation of Northern China and India. Prog Nat Sci 16:980–985

Wang YM, Li SL, Luo DH (2009) Seasonal response of Asian monsoonal climate to the Atlantic Multidecadal Oscillation. J Geophys Res 114:D02112. doi:10.1029/2008JD010929

Wei FY, Hu L, Chen GJ, Li Q, Xie Y (2012) Reconstruction of summer sea level pressure over east Asia since 1470. J Clim 25:5600–5611

Wigley TML, Briffa KR, Jones PD (1984) Average value of correlated time series, with applications in dendroclimatology and hydrometeorology. J Appl Meteorol Clim 23:201–234

Wilhite DA (2000) Drought as a natural hazard: concepts and definitions. In: Wilhite DA (ed) Droughts: global assessment. Routledge, London, pp 3–18

Wu B, Zhou TJ, Li T (2009) Seasonally evolving dominant interannual variability modes of East Asian climate. J Clim 22:2992–3005

Xiao SC, Xiao HL, Peng XM, Tian QY (2014) Daily and seasonal stem radial activity of Populus euphratica and its association with hydroclimatic factors in the lower reaches of China's Heihe River basin. Environ Earth Sci 72:609–621. doi:10.1007/s12665-013-2982-y

Yi L, Yu H, Ge J, Lai Z, Xu X, Qin L, Peng S (2012) Reconstructions of annual summer precipitation and temperature in north-central China since 1470 AD based on drought/flood index and tree-ring records. Clim Chang 110:469–498

Zhang R, Delworth TL (2007) Impact of the Atlantic multidecadal oscillation on North Pacific climate variability. Geophys Res Lett 34:L23708. doi:10.1029/2007GL031601

Zhang Q, Gao G (2004) The spatial and temporal features of drought and flood disasters in the past 50 years and monitoring and warning services in China. Sci Technol Rev 7:21–24

Zhang DE, Liang YY (2010) A long lasting and extensive drought event over China during 1876–1878 (in Chinese). Adv Clim Change Res 6:106–112

Zhang R, Sumi A, Kimoto M (1999) A diagnostic study of the impact of El Nino on the precipitation in China. Adv Atmos Sci 16:229–241

Zhang P, Cheng H, Edwards RL, Chen F, Wang Y, Yang X, Liu J, Tan M, Wang X (2008) A test of climate, sun, and culture relationships from an 1810-year Chinese cave record. Science 322:940–942

Zhao XL, Li WY (1963) Mongolian Scotch Pine. Agriculture Press, Beijing, pp 71–73 (In Chinese)

Zhao HL, Zhao XY, Zhang TH, Zhou RL (2002) Boundary line on agro-pasture zigzag zone in north China and its problems on eco-environment. Adv Earth Sci 17:739–747

Zhu JJ, Fan ZP, Zeng DH, Jiang FQ, Matsuzaki T (2003) Comparison of stand structure and growth between artificial and natural forests of Pinus sylvestiris var. mongolica on sandy land. J For Res 14:103–111

Zou XK, Zhai P, Zhang Q (2005) Variations in droughts over China: 1951–2003. Geophys Res Lett 32:L04707